POLITECNICO DI TORINO
Repository ISTITUZIONALE

Fatigue Load Reduction and Variable-Structure Control Techniques for DFIM-based Wind Farm Scenarios

Original
Fatigue Load Reduction and Variable-Structure Control Techniques for DFIM-based Wind Farm Scenarios / Cacciolatto, A.; Capello, E.; Wada, T.; Fujisaki, Y.. - ELETTRONICO. - 53:(2020), pp. 12656-12662. (Intervento presentato al convegno IFAC World Congress 2020) [10.1016/j.ifacol.2020.12.1845].

Availability:
This version is available at: 11583/2897954 since: 2021-05-03T18:13:01Z

Publisher:
Elsevier

Published
DOI:10.1016/j.ifacol.2020.12.1845

Terms of use:

This article is made available under terms and conditions as specified in the corresponding bibliographic description in the repository

Publisher copyright
Elsevier postprint/Author's Accepted Manuscript

© 2020. This manuscript version is made available under the CC-BY-NC-ND 4.0 license http://creativecommons.org/licenses/by-nc-nd/4.0/.The final authenticated version is available online at: http://dx.doi.org/10.1016/j.ifacol.2020.12.1845

(Article begins on next page)

12 October 2024

Available online at www.sciencedirect.com

ScienceDirect

IFAC PapersOnLine 53-2 (2020) 12656–12662

Fatigue Load Reduction and Variable-Structure Control Techniques for DFIM-based Wind Farm Scenarios

A. Cacciolatto * **E. Capello** ** **T. Wada** *** **Y. Fujisaki** ***

* *Formerly, Department of Control and Computer Engineering, Politecnico di Torino, Torino, Italy*

** *Department of Mechanical and Aerospace Engineering, Politecnico di Torino, and with Institute of Electronics, Computer and Telecommunication Engineering, National Research Council of Italy (CNR-IEIIT), Torino, Italy*

*** *Department of Information and Physical Sciences, Osaka University, Suita, Japan*

Abstract: This paper proposes a trade-off approach between fatigue reduction and power extraction for wind farm scenarios, in which a simplified model for a Horizontal Axis Wind Turbine is developed. Both the aerodynamics and the electrical-mechanical model are implemented, considering a Doubly-Fed Induction Machine (DFIM). This model is controlled and connected to the grid by a back-to-back converter, composed of two bi-directional voltage source inverters . Moreover, the stator windings of the generator are directly linked to the grid and the rotor windings are connected to the grid through the power converter. The control of the VSIs is based on super-twisting sliding mode control, which guarantees robustness and low chattering effects. A wake model and an optimization problem for the reduction of the loads are included, to reduce the maximum fatigue load without compromising the power extraction. The results show a performance tracking of a desired rotational speed for the DFIMs and reduction of fatigue and damage, with a limited power reduction compared with the maximum power point tracking.

Copyright © 2020 The Authors. This is an open access article under the CC BY-NC-ND license (http://creativecommons.org/licenses/by-nc-nd/4.0)

Keywords: Sliding mode control, Energy systems, Control of renewable energy resources, Control system design, Renewable Energy System Modeling.

1. INTRODUCTION

Maximizing the energy production is the main issue design in renewable systems, such as wind farms. However, in the last years, a trade-off between the energy production and system performance in terms of mechanical loads is the main objective of the control systems. Indeed, advanced controllers are hidden technologies, which can contribute to harvesting as much wind energy as possible and converting it to electricity while keeping maintenance costs low, increasing the system performance. In this paper the control objectives are twofold: (i) reference tracking error minimization and (ii) mechanical stress reduction, including the electro-mechanical model of the wind turbine and the wake model interaction. Surveys on control of wind farm and wind turbines, as in (Rezaei, 2015; Knudsen et al., 2015), focus on methodologies for power production, fatigue reduction and wakes affecting neighbouring wind turbines.

Modeling and control of wind turbines are difficult tasks, since it is a complex structure that includes different subsystems with nonlinear and time-varying behavior. In (Rezaei, 2015), different control methodologies are proposed, based on nonlinear control theory (i.e. (Schlipf et al., 2013; Saravanakumar and Jena, 2016; Song et al., 2017)), on robust control methods (i.e. (Moradi and Vossoughi, 2015; Simani and Castaldi, 2018; Singh et al., 2018)) or on sliding mode control theory (i.e. (Liu et al., 2018; Yang and Tan, 2019)). In the last years, different control schemes, based on variable structure control systems, as sliding mode control (SMC) systems, are designed by researchers. For example, in (Hong et al., 2014) the effectiveness of a robust sliding mode controller is verified with a single turbine, including doubly-fed induction generator (DFIG) model. In similar way, in (Gajewski and Pieńkowski, 2017) a sliding mode controller for the tracking of the MPPT operating points is proposed, in which the effectiveness of the control strategy in wind energy conversion system is proven with direct-driven in Permanent Magnet Synchronous Generator. In (Ebrahimkhani, 2016) a fractional order SMC control systems is proposed focusing on maximum power point tracking (MPPT) control of a wind turbine. In our paper a super-twisting (STW) sliding mode controller (SMC) (Levant, 1993) is selected to guarantee high efficiency and robustness to parametric uncertainties, for a wind farm scenario. Moreover, the STW sliding mode approach is designed for the electro-mechanical system of the wind turbine, showing a reduction of mechanical stress since no strong torque variations are required. Traditionally, wind farm is operated as a collection of individually controlled wind turbines (Heer et al., 2014) and, if the wind turbine is individually controlled, it usually works at its locally optimal operating point, which assures maximum available power from (which is called maximum power point tracking (MPPT)). However, due to the aerodynamic interactions, the strategy of having each wind turbine in an array extract as much power as possible does not lead to our control objectives. One of the key feature here proposed is the improvement of the efficiency of the wind

2405-8963 Copyright © 2020 The Authors. This is an open access article under the CC BY-NC-ND license.
Peer review under responsibility of International Federation of Automatic Control.
10.1016/j.ifacol.2020.12.1845

power conversion systems, i.e. wind farm scenario, by using an appropriate control algorithm.

This work is based on the previous researches described in (Capello et al., 2018; Capello et al., 2018; Capello et al., under review). The contributions of this work with respect to these previous works are: (i) a detailed model of the electro-mechanical system of the turbine, (ii) a control system designed for the mechanical and electrical parts of the turbine, (iii) an optimization problem in which three objectives are implemented: maximization of the power extraction, minimization of the extreme loads and fatigue loads. The effectiveness of the proposed approach is shown for a wind farm including four turbines, affected by wake interactions. The results obtained with our method are compared with the MPPT operation point.

The paper is organized as follows. The overview of wind farm main features and the model of a wind farm is introduced in 2. In detail, in Section 2.3, the wind turbine electro-mechanical model is deeply described. In the remainder of the Section, power coefficient evaluation and wake interaction model are described. Section 3 proposes the STW sliding mode controller suitably designed for tracking the desired operating points. In Section 4, the optimization problem is defined for the evaluation of the operating points. Some preliminary results for a wind farm scenario are presented in 5, including aerodynamic interference and comparison with the maximum power point tracking. Finally, some concluding remarks are described in Section 6.

2. WIND FARM SCENARIO AND WIND TURBINE MODEL

Starting from the definitions in (Pao and Johnson, 2009), we are focusing on Region 2 operation mode, in which a variable speed wind turbine captures the most power possible from the wind. Moreover, in Region 2 the wind speed range is from 5 to 14 m/s. In our scenario, wind trubines in a wind farm are located within a relatively small area (Fig. 1), then an electro-mechanical model of the wind turbine and the wake interaction model are also included. Each wind turbine extracts a part of the energy from the wind flow. This causes decrease in wind speed after the turbine and introduces aerodynamic interactions and wind speed deficits for subsequent turbines. This variation of the wind speed is evaluated in Section 2.1.

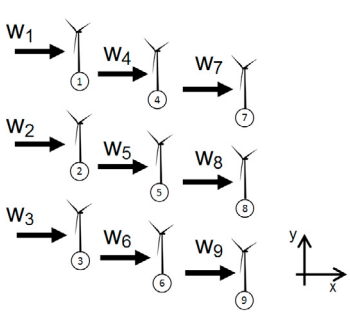

Fig. 1. Wind Farm Scenario

In this paper, the electro-mechanical model of the wind turbine is deeply introduced in the Section 2.3. The mathematical model can be organized in the following subsystems:

- The wind and wake interactions (Section 2.1)
- The wind turbine aerodynamics and gearbox for the mechanical transmission of power (Section 2.2)
- The doubly-fed induction machine (DFIM) and related power converter (Section 2.3)

For the purpose of this research, the input wind is considered fixed in direction, as in Fig. 1. Moreover, the changes on wind direction imply a control system of the nacelle yaw angle, in order to guarantee a wind direction perpendicular to the turbine rotating blades. This control loop and modeling is out of the scope of this paper.

We assume that the wind speed is measured by a sensor (i.e. LIDAR sensor), which is installed in the first turbine of the wind farm scenario. So, the wind speed on the first turbine is measured by the sensor and it is not affected by the wake interactions, instead the wind speed in the other turbines of the wind farm is estimated with the Jensen wake model.

2.1 Wind and Wake Interaction Model

The wind speed, which is responsible for both the wakes and the electro-mechanical conversion, is modeled as combination of (1) a constant value w_{const} which is included in the range of Region 2, (2) a low-frequency sinusoidal value which corresponds to fluctuations of the wind speed over long periods of time $w_{l,sin}$, (3) a high-frequency sinusoidal value which is fluctuations of the wind speed over short periods of time $w_{h,sin}$, and (4) a random white noise signal which represents the measurement uncertainties w_{noise}. The last three components vary during the simulations, instead w_{const} is fixed and refers to the average value of the considered wind speed. Now, the wind speed is modeled as

$$\tilde{w}_i = w_{const,i} + w_{l,sin,i} + w_{h,sin,i} + w_{noise,i},$$

for $i = 1, 2, \ldots, n$, where n is the number of turbines in the wind farm. This model is selected to show the robustness of the proposed control technique.

The wake model chosen for this research is known as the Jensen/Park model (Jensen, 1983). This model is a kinematic, parametric, and static model based on the actuator disk model theory (Johnson, 1980). The main assumptions of this last theory are (i) linear expansion of the wake and (ii) superposition effect of multiple wakes acting on a turbine. Moreover, it is based on the assumption of a wake with linearly expanding diameter.

Starting from definition of the power and torque coefficients (7) can be derived that

$$1 - 2a_i = \sqrt{1 - C_{T,i}}, \tag{1}$$

where a_i and $C_{T,i}$ are the axial induction factor and the torque coefficient of the i-th turbine, respectively. Assuming a linear expansion, the linear dimension (radius R) is proportional to the down-wind distance x, as in the following equation

$$R(x) = R + \alpha x. \tag{2}$$

As explained in González-Longatt et al. (2012), α is defined as the decay coefficient and it is set to 0.075 for onshore, and to 0.05 for offshore wind farms, see Fig. 2 in which $R(x)$ is defined.

The wind speed in the wake at distance x from the turbine can be computed as

$$w_i(x) = \tilde{w}_i \left[1 - (1 - \sqrt{1 - C_{T,i}}) \left(\frac{R}{R(x)} \right)^2 \right]. \tag{3}$$

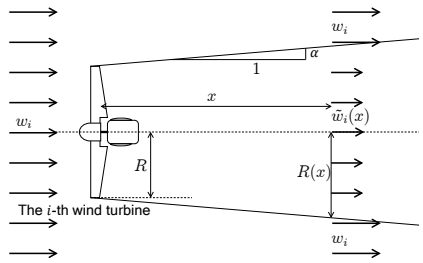

Fig. 2. Linear expansion of the wake assumed in the Jensen wake model, starting from (González-Longatt et al., 2012)

For detailed model of the wake interaction, refer to González-Longatt et al. (2012) and Capello et al. (under review). Applying the superposition effect, the complete model for the input wind speed of a turbine is

$$w_i = w_\infty \left[1 - (1 - \sqrt{1 - C_{T,i}}) \sum_{j=1, j\neq i}^{n} \left(\frac{R}{R(x_{ij})} \right)^2 \frac{A_{sh,ij}}{A_0} \right]. \quad (4)$$

This shadowing is a measure of the degree of overlap between the area defined by the wakes shadow cone ($A_{sh,ij}$) and the area swept by the turbine experiencing shadowing ($A_0 = \pi R^2$). The shadowing areas, as previously said, are not described here in detail. In our systems, the number of wind turbines and the layout of the wind farm are known, thus the wake interactions between turbines are known a priori. Moreover, we assume $w_1 = w_\infty$, since the first turbine is not affected by wake interaction.

2.2 Wind Turbine Aerodynamics

For the evaluation of the power extraction, the power coefficient C_P is defined as the ratio of actual mechanical power produced by a wind turbine divided by the total wind power flowing into the turbine blades at specific wind speed. The main idea of the energy extraction from the wind is caused by the capture of the kinetic energy from the wind, that is limited by the Betz law (Ragheb and Ragheb, 2011). This law defines the maximum value for the power coefficient C_P, to which corresponds a maximum value for the axial induction factor. The axial induction factor a_i (Johnson, 1980) is also defined as the velocity reduction relative to the free wind speed:

$$a_i = \frac{w_\infty - w_i}{w_\infty}, \quad (5)$$

where w_∞ is the wind speed not affected by aerodynamic interactions and w_i is the speed acting on the turbine. From the axial induction factor definition, the power and torque coefficients are respectively the percentage of power extracted by the wind turbine from the wind resource and the torque acting on the turbine, that is,

$$C_{P,i} = 4a_i(1 - a_i)^2, \quad (6)$$

$$C_{T,i} = 4a_i(1 - a_i). \quad (7)$$

The speed w_i is function of the speed acting on the first turbine (i.e. the flow speed w_∞) and it is affected by aerodynamic interactions (deeply discussed in Section 2.1).

Moreover, the power coefficient C_P can be defined as a function of λ and β as follows

$$C_P(\lambda, \beta) = c_1 \left(\frac{c_2}{\bar{\lambda}} - c_3\beta - c_4 \right) e^{\frac{-c_5}{\bar{\lambda}}}, \quad (8)$$

$$\frac{1}{\bar{\lambda}} = \frac{1}{\lambda + 0.08\beta} - \frac{0.035}{\beta^3 + 1}, \quad (9)$$

where the angles are expressed in degrees (Heier, 1998; Rosyadi et al., 2012) and the coefficients $c_1, c_2, \ldots, c_5$ depend on the wind turbine's design and aerodynamic characteristics.

For the wind turbine control problem, the optimal operating point is evaluated from the optimal angular rotation speed ω_{opt},

$$\omega_{\text{opt}} = \frac{\lambda_{\text{opt}} w}{R}, \quad (10)$$

where λ_{opt} is computed with an optimization algorithm, such as (i) the MPPT tracking, which leads to the maximum extraction of mechanical power or (ii) a more conservative approach, as presented here (Barradas-Berglind and Wisniewski, 2016). The wind speed w_i is affected by aerodynamic interactions.

For both cases, the pitch angle β is considered as a constant, since the turbines are operating in Region II. A variable wind speed behavior is included in the model starting from the model described in Safari (2011) and including random noise. The reference angular velocity, to be tracked by the controller for the generator, is evaluated as

$$\omega_{ref} = K_{prop} N \omega_{opt}, \quad (11)$$

where N is a gear ratio (constant) and K_{prop} is a proportional gain to compensate the errors in the model and the efficiency of the gearbox.

For the wind farm scenario, the total power extraction $P_{g,i}$ of each turbine should be easily written in function of the axial induction factor a_i.

$$P_{a,i}(a_i, w_i) = \frac{1}{2}\rho\pi R^2 w_i^3 a_i (1 - a_i)^2 \quad (12)$$

where ρ is the air density, R is the radius of the turbine and w_i is the speed acting on the turbine.

Summarizing, we have that $C_{P,\max} = 16/27 \approx 0.59$ and $a_{\max} = 1/3$. This equation can be translated in

$$C_{P,i} = 4a_i(1 - a_i)^2 = \frac{P_{\text{mech},i}}{P_{\text{wind},i}}, \quad (13)$$

where $P_{\text{wind},i}$ is the maximum power extracted from the i-th wind turbine and $P_{\text{mech},i}$ is the mechanical power, that cannot be more than 59% of $P_{\text{wind},i}$. In real applications, this value is reduced due to unmodeled dynamics and energy losses in the actuator disk model. Notice that the values of the coefficients (8) depends on the wind turbine design, that is, λ and β are control parameters for speed regulation and power production.

Since the wind perturbation could lead to outage of a wind turbine, intensity of turbulence effect at i-th wind turbine is modeled as $I_{\text{eff},i} = \frac{\hat{\sigma}_i}{w_i}$. $I_{\text{eff},i}$ is effective turbulence intensity which corresponds to fatigue risk of the wind turbine, where $\hat{\sigma}_i$ is a characteristic ambient turbulence standard deviation of the input wind speed to the i_{th} turbine, w_i is the average wind speed, which is updated with a frequency of 1 Hz in accordance to the Jensen wake model (see next Section).

The turbulence effect cannot be described by means of the actuator disk model in its standard form due to the many ideal hypothesis assumed. For this reason, we use the polynomial approximation proposed by Barradas-Berglind and Wisniewski (2016), in which the fatigue damage is modeled as

$$D_i(a_i, w_i) = c w_i^2 I_{\text{eff},i}^2 (z_2 a_i^2 + z_1 a_i + z_0), \quad (14)$$

where w_i is the wind speed acting on the i-th turbine, $I_{\text{eff},i}$ is defined before, and $c = 2\rho A$. The polynomial coefficients are

obtained from Barradas-Berglind and Wisniewski (2016) such as $z_2 = 127.5$, $z_1 = -12.41$ and $z_0 = 4.65$. The wind speed variation is evaluated including the aerodynamic interactions, that will be described in the next Section. In a similar way, the fatigue can be defined as function of the axial induction factor and the wind speed.

$$F_i(a_i, w_i) = 2\rho A_0(4a_i(1 - a_i))w_i^2, \tag{15}$$

where $A_0 = \pi R^2$ is the disk area of the i-th turbine, a_i is the axial induction factor of the i-th turbine and w_i is the wind speed acting on the i-th turbine, as before.

2.3 Wind Turbine Electrical Drive

A simplified model for an Horizontal Axis Wind Turbine (HAWT) has been developed considering both the aerodynamics and the electrical generator. This last one has been developed considering a Doubly-Fed Induction Machine (DFIM), which is controlled and connected to the grid by a back-to-back converter. Two bi-directional voltage source inverters (VSIs) are included, where the stator windings of the generator are directly linked to the grid and the rotor windings are connected to the grid through the power converter. This configuration is the most used in industrial applications for its efficiency, reduced costs and reliability.

Before describing the control scheme for the DFIM, some fundamental laws describing the behaviour of the electrical machine itself are briefly introduced. The starting point is the relationship between the magnetic field at the stator (constant in amplitude and frequency) and the magnetic field at rotor and the rotational speed of the rotor itself. In fact, the DFIM is by definition an asynchronous system, which means that the magnetic field of the stator and the rotational speed of the rotor are not the same. A description of the phenomenon can be found in Fletcher and Yang (2010), while the the equations describing the behaviour of the electrical machine are taken from Abad and Iwanski (2014).

In a similar way, the grid system has to be modeled in order to properly design the control system for the grid side converter. A model based design approach is selected and implemented, including a series of blocks imported from the Simscape power system library. The electrical equations of the asynchronous machine are in Mekrini and Bri (2016); Aktaibi et al. (2011).

3. SECOND-ORDER SLIDING MODE CONTROLLER

Sliding mode is a nonlinear control approach, which is able to ensure high accuracy and excellent robustness against external disturbances and parameter variations with simple design. For this application, a STW algorithm (Levant, 1993) is selected, since it is a second order SMC and it is a continuous controller. Moreove, it is able to provide all the main properties of SMC for systems affected by smooth matched uncertainties/disturbances with bounded gradients. As well explained in (Capello et al., 2018; Barambones and Gonzalez de Durana, 2015), sliding mode control is demonstrated to be very effective for WT systems, due to its robustness to uncertainties in the wind model definition and to show a *smooth* control input.

In order to produce active power at a desired rotational speed, the main goals of the proposed control scheme are

(1) maintaining a desired voltage on the DC-link in the AC-DC-AC converter,

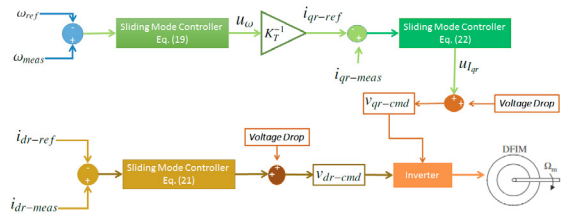

Fig. 3. The proposed control scheme

(2) keeping the reactive power production as low as possible, to reduce loss of extracted power,
(3) tracking a desired rotational speed, while the wind imposes a torque on the shaft of the generator.

In order to achieve these goals, a double loop control structure is proposed in which both electrical and mechanical parameters are controlled. This approach is the nowadays standard for most of the electrical systems. More details on the control scheme proposed for the DFIM are here described. This double control loop is in Figure 3.

The main control objective is to enhance the captured power and the efficiency, while reducing mechanical fatigue and attenuating the output chattering. The outer loop of the speed control is

$$\begin{cases} u_\omega = -A_{w1}|\omega_{meas} - \omega_{ref}|^{\frac{1}{2}} sign(\omega_{meas} - \omega_{ref}) + u_1 \\ \dot{u}_1 = -A_{w2} sign(\omega_{meas} - \omega_{ref}) \end{cases}, \tag{16}$$

where $\omega_{ref} = K_{prop} N \omega_{opt}$ as in Eq. (11). The output of the speed controller is, by definition, the electromagnetic torque, that mechanically opposes the mechanical torque in input coming from the wind turbine shaft. Note that the current reference value for the inner control loop is

$$i_{qr-ref} = -\frac{2u_\omega}{3pF_s \frac{Lm}{Ls}} = u_\omega K_T^{-1}. \tag{17}$$

as in the scheme of Figure 3, where $K_T = -\frac{2}{3pF_s \frac{Lm}{Ls}}$ is function of the electrical system.

In a similar way, the current regulators have the following control scheme,

$$\begin{cases} u_{I_{dr}} = -A_{1dr}|i_{dr-meas} - i_{dr-ref}|^{\frac{1}{2}} sign(i_{dr-meas} - i_{dr-ref}) + u_1 \\ \dot{u}_1 = -A_{2dr} sign(i_{dr-meas} - i_{dr-ref}) \end{cases},$$

$$\begin{cases} u_{I_{qr}} = -A_{1qr}|i_{qr-meas} - i_{qr-ref}|^{\frac{1}{2}} sign(i_{qr-meas} - i_{qr-ref}) + u_1 \\ \dot{u}_1 = -A_{2qr} sign(i_{qr-meas} - i_{qr-ref}) \end{cases}.$$

The final values for the inputs are defined following the voltage laws described before. Note that the voltage drop on the resistance has been neglected, $v_{dr-cmd} = u_{I_{d-r}} - (2\pi f - p\omega_m)L_r i_{qr-1}$ and $v_{qr-cmd} = u_{I_{q-r}} + (2\pi f - p\omega_m)\sigma L_r i_{dr-meas} + (2\pi f - p\omega_m)\frac{L_m}{L_s}F_s$.

4. OPTIMIZATION PROBLEM

In this section, we describe an optimization problem for achieving maximization of the total power generation and minimization of fatigue risks and extra stress to towers of wind turbines. Based on previous results of some of the authors (Capello et al., 2018; Capello et al., 2018, under review), an optimization problem, which considers three objectives for a general shaped wind farm, as in (Barambones and Gonzalez de Durana, 2015),

is here proposed. Furthermore, we explain this method from a viewpoint of multi-objective optimization.

We have three objectives. The first one is maximization of the total extracted power in the wind farm. The objective function is given by

$$J_P(a, w) = \sum_{i=1}^{n} P_{g,i}(a_i, w_i),$$

where $a \in \mathbb{R}^n$ is a vector whose component a_i is axial induction factor at i-th wind turbine and $w \in \mathbb{R}^n$ is a vector which consists of wind speed at each wind turbine. $P_{g,i}$ is the extracted power described by Eq. (11). The second objective is the total extreme loads on the turbines' towers

$$J_F(a, w) = \sum_{i=1}^{n} F_i(a_i, w_i),$$

where F_i is given by Eq. (15). The last one is the total fatigue damage

$$J_D(a, w) = \sum_{i=1}^{n} D_i(a_i, w_i).$$

The function D_i is also determined by Eq. (14).

Our goal in optimization is maximization of the total power generation, minimization of the total extreme loads on turbine towers, and minimization of the total fatigue damage, simultaneously. That is, we can formulate our problem as a multi-objective optimization:

$$\max_a J_P(a, w),\ -J_F(a, w),\ -J_D(a, w),$$

for a given wind speed vector w. To solve the above multi-objective optimization, we consider the optimization:

$$\max_a \quad J(a, w) = J_P - \zeta J_f - \chi J_d \tag{18a}$$

$$\text{s.t.} \quad 0 < a_i < 1/3, \quad i = 1, 2, \ldots, n \tag{18b}$$

for given positive parameters $\zeta \geq 0$ and $\chi \geq 0$. That is, we seek for a Pareto-optimal solution of the multi-objective optimization problem. In this optimization, the constraint conditions correspond to the Betz limit (Johnson, 1980). The problem includes the Maximum Power Point Tracking (MPPT) case as a special case. In fact, when we select $\zeta = \chi = 0$, the optimization problem is the MPPT case.

Remark 1. In the optimization, we need information on wind speed w at each wind turbine. One approach is to estimate wind speed based on wake interaction model such as Jensen/Park model. Another approach is to measure wind speed by sensors. In Section 5, we assume that we can measure wind speed at the first two turbines and we solve the optimization every 35 seconds. The wind speed in the turbines 3 and 4 are estimated by Jensen model (updated each 1 second). When we solve it, we employ average wind speed under previous time intervals.

From the induction factors, we determine reference tip speed ratios λ_i and reference pitch angles β_i, $i = 1, 2, \ldots, n$. Now, please recall that the power coefficient is also a function of the tip-speed ratio and the pitch angle as shown in Eq. (8). That is, tip speed ratios and pitch angles satisfying

$$\min_{\lambda_i \geq 0} \ \lambda_i \quad \text{s.t.} \ C_P(\lambda_i) = C_{P,i}(a_i).$$

for $i = 1, 2, \ldots, n$, are reference tip speed ratio and pitch angle of each wind turbine.

At last, we determine reference rotational speed $\omega_{\text{ref},i}$ of the DFIM from λ_i. The gear ratio N and a proportional constant K_{prop} which represents the unmodeled dynamics of the system, the rotor radius R, and the wind speed w_i lead to

$$\omega_{\text{ref},i} = K_{\text{prop}} N \frac{\lambda_i w_i}{R}.$$

Remark 2. In simulations, we assume that the pitch angle is fixed as a constant value. This is because we focus on Region 2 of operating mode of wind turbines. Furthermore, we utilize an approximation of (8) for solving the optimization problem easily. In fact, we employed the following approximation:

$$\begin{aligned} &C_P(\lambda, \beta) \\ &= C_P(\lambda) = -0.0022\lambda^3 + 0.0218\lambda^2 + 0.0267\lambda - 0.0437. \end{aligned}$$

in next section.

5. SIMULATION RESULTS

A simple scenario of four turbines is simulated, as in Fig. 4, in which the first two turbines are affected by the nominal wind speed ($w_1 = w_\infty$) and the other two turbines have a reduced wind speed, in accordance to the Jensen model. Four NREL 1.5 MW turbines (Pao and Johnson, 2009) are included. The rotor radius is $R = 35$ m and $A_0 = 3.85 \cdot 10^3$ m^2. A simulation of 300 s is performed in MATLAB/Simulink, with a fixed-step sample frequency of 1000 Hz and ode4 solver. As previously introduced, the model of a doubly fed induction generator, the relative power conversion system and the grid connection system are included in the simulator, with the help of the Simscape libraries. In detail, in order to design the electrical system for the wind turbines, a model based design approach is proposed, in which some blocks, imported from the Simscape power system library, are included.

Both the wind farm model and the sliding mode controllers are updated with a frequency of 1000 Hz. The Jensen model (i.e. the wake model) is updated with a frequency of 1 Hz, since the undisturbed wind speed is assumed to be measured with a LIDAR sensor and we imagine to store the measurements with a limited frequency. Moreover, each 35 seconds the optimization problem is run, to evaluate new set-points for the wind turbines. The pitch angle β of the turbines is fixed and equal to 0.5 deg. The nominal rotational speed (DFIG shaft) is $\omega_n = 1500$ rpm and the gear ratio $N = 10$. The average wind speed w_{const} applied to the wind farm is 12 m/s. The results

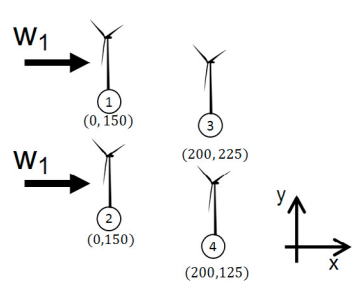

Fig. 4. Wind farm scenario

obtained with the proposed optimization problem are compared with the MPPT point, with an induced factor $a = a_{mppt}$.

MPPT Tracking Results. The MPPT solution has an induced axial factor of $a = 0.33$ for all the turbines, tip speed ration $\lambda = 6.3026$, and a fixed pitch angle $\beta = 0.5$ deg. After the

definition of these parameters, the optimum angular speed for each wind turbines is

$$\omega_{\text{mppt},i} = \frac{\lambda_{\text{mppt}} w_i}{R},$$

where w_i is the wind speed evaluated with the wake model (as described in Section 2.1) for the ith turbine and R is the radius of the ith turbine. In the selected wind farm configuration, all the turbines have the same radius, $R = 35$ m.

For this case, the maximum total power produced by the wind farm is $P_{g,\text{mppt}} = 1.13 \cdot 10^7$ W and the maximum fatigue value is $F_{\text{max,mppt}} = \sum_{i=1}^{n} F_i = 5.787 \cdot 10^6$ N. Finally, the damage is evaluated for the wind farm as previously indicated and the maximum value is $D_{\text{max,mppt}} = \sum_{i=1}^{n} D_i = 1.506 \cdot 10^5$ N.

Fatigue Reduction Tracking Results. For the fatigue reduction tracking, the main objective is the combination of the control system and the optimization problem for the fatigue evaluation, including aerodynamic interactions. The aerodynamic interactions are evaluated with a reduced frequency (1 Hz) and the optimization problem, in order to reduce the computational effort of the system, is performed each 35 seconds. The axial factors and the effective turbulence intensity are evaluated with an optimization problem, including only 4 turbines (as in Fig. 4).

The maximum value of fatigue for the optimized problem is $F_{\text{max,opt}} = \sum_{i=1}^{n} F_i = 5.436 \cdot 10^6$ N, with a loss of fatigue of about 6% with respect to the MPPT case. The comparison is in Figure 6.

As previously stated, power extraction is reduced and, in the analyzed case, we have a reduction of the total power generated by about 1%. In detail, the maximum power produced is $P_{g,\text{opt}} = 1.157 \cdot 10^6$ W. In Fig. 7 it is possible to observe a damage reduction of about 16%. The total power produced is compared with the power extracted tracking the MPPT point for a simulation of 300 seconds. As in Fig. 5, the extracted power is similar in the two operating points, but a reduction of fatigue is guaranteed with the proposed approach, as well as the damage.

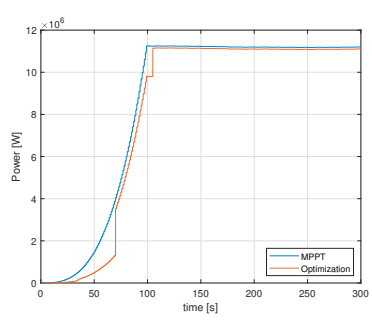

Fig. 5. Comparison of extracted power between MPPT case and the optimized problem

The STW-SMC control system is able to track the angular velocity obtained with the optimization problem, as in the previous case. The error of the angular velocity is evaluated for the first turbine after 10 s of simulation and it is about 10^{-3} rpm.

6. CONCLUSION

A trade-off between the extracted power and the fatigue loads for a wind farm scenario is proposed in this paper, including interference raising among the wind turbines. The wind turbine dynamics includes the model of doubly-fed induction generator and mechanical stresses, to show the effectiveness of the proposed control strategy. Two second-order sliding mode controllers are designed for the control of both the rotor-side and grid-side converters. A minimization of the fatigue loads with a minimum loss of power extraction is shown for a simple scenario. The optimization problem guarantees that the power extraction is similar to the maximum power point tracking, but a reduction of damage and fatigue is observed. A low computational effort of the proposed solution is guaranteed, with a reduction of update frequencies of the optimization problem and of the wake interaction model. Future works will include a more detailed model of the wind and parametric uncertainties on the wind turbine model.

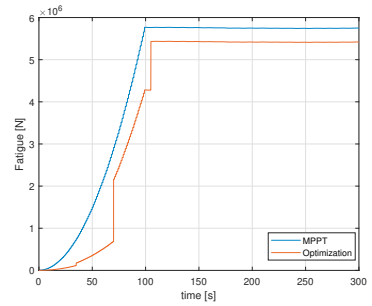

Fig. 6. Comparison of fatigue value $F = \sum_{i=1}^{4} F_i$ between MPPT case and the optimized problem

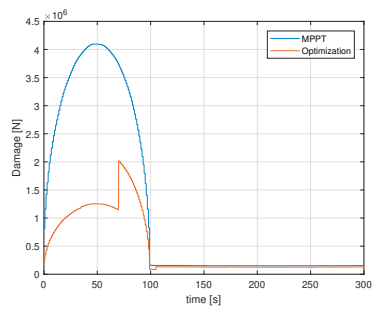

Fig. 7. Comparison of damage $D = \sum_{i=1}^{4} D_i$ between MPPT case and the optimized problem

ACKNOWLEDGEMENTS

The authors would like to thank Dr. Elisabetta Punta for the insightful discussions on Sliding Mode Controller and wind farm applications. This work was supported by COOPS, International Bilateral Joint CNR Laboratories, and JST CREST Grant Number JPMJCR15K2, Japan.

REFERENCES

Abad, G. and Iwanski, G. (2014). Properties and control of a doubly fed induction machine. *Power Electronics for Renewable Energy Systems, Transportation and Industrial Applications*, 270–318.

Aktaibi, A., Ghanim, D., and Rahman, M. (2011). Dynamic simulation of a three-phase induction motor using matlab simulink.

Barambones, O. and Gonzalez de Durana, J.M. (2015). Wind turbine control scheme based on adaptive sliding mode con-

troller and observer. In *2015 IEEE 20th Conference on Emerging Technologies Factory Automation (ETFA)*, 1–7.

Barradas-Berglind, J.J. and Wisniewski, R. (2016). Wind farm axial-induction factor optimization for power maximization and load alleviation. In *2016 European Control Conference (ECC)*, 891–896.

Capello, E., Wada, T., Punta, E., and Fujisaki, Y. (2018). Minimax optimization of fatigue loads in a wind farm and its realization via sliding mode controller of wind turbines. In *2018 IEEE Conference on Control Technology and Applications (CCTA)*, 430–435.

Capello, E., Wada, T., Punta, E., and Fujisaki, Y. (2018). Wind farm sliding mode control and energy optimization with fatigue constraints. In *SICE International Symposium on Control Systems 2018*.

Capello, E., Wada, T., Punta, E., and Fujisaki, Y. (under review). Optimization of fatigue loads and sliding mode technique for wind farm scenarios. *IET Contrl Theory & Applications*.

Ebrahimkhani, S. (2016). Robust fractional order sliding mode control of doubly-fed induction generator (dfig)-based wind turbines. *ISA Transactions*, 63, 343 – 354.

Fletcher, J. and Yang, J. (2010). Introduction to doubly-fed induction generator for wind power applications. *Paths to Sustainable Energy*, 259–278.

Gajewski, P. and Pieǹkowski, K. (2017). Analysis of sliding mode control of variable speed wind turbine system with pmsg. In *2017 International Symposium on Electrical Machines (SME)*, 1–6.

González-Longatt, F., Wall, P., and Terzija, V. (2012). Wake effect in wind farm performance: Steady-state and dynamic behavior. *Renewable Energy*, 39(1), 329–338.

Heer, F., Esfahani, P.M., Kamgarpour, M., and Lygeros, J. (2014). Model based power optimisation of wind farms. In *2014 European Control Conference (ECC)*, 1145–1150.

Heier, S. (1998). *Grid Integration of Wind Energy Conversion Systems*. Wiley.

Hong, C.M., Huang, C.H., and Cheng, F.S. (2014). Sliding mode control for variable-speed wind turbine generation systems using artificial neural network. *Energy Procedia*, 61, 1626 – 1629. International Conference on Applied Energy, ICAE2014.

Jensen, N.O. (1983). A note on wind generator interaction. Technical report, Risø National Laboratory for Sustainable Energy, Technical University of Denmark.

Johnson, W. (1980). *Helicopter Theory*. Dover.

Knudsen, T., Bak, T., and Svenstrup, M. (2015). Survey of wind farm control—power and fatigue optimization. *Wind Energy*, 18(8), 1333–1351.

Levant, A. (1993). Sliding order and sliding accuracy in sliding mode control. *International journal of control*, 58(6), 1247–1263.

Liu, Y., Wang, Z., Xiong, L., Wang, J., Jiang, X., Bai, G., Li, R., and Liu, S. (2018). Dfig wind turbine sliding mode control with exponential reaching law under variable wind speed. *International Journal of Electrical Power & Energy Systems*, 96, 253–260.

Mekrini, Z. and Bri, S. (2016). A modular approach and simulation of an asynchronous machine. *International Journal of Electrical and Computer Engineering (IJECE)*, 6, 1385–1394.

Moradi, H. and Vossoughi, G. (2015). Robust control of the variable speed wind turbines in the presence of uncertainties: A comparison between h∞ and pid controllers. *Energy*, 90, 1508–1521.

Pao, L.Y. and Johnson, K.E. (2009). A tutorial on the dynamics and control of wind turbines and wind farms. In *2009 American Control Conference*, 2076–2089.

Ragheb, M. and Ragheb, A.M. (2011). Wind turbines theory-the betz equation and optimal rotor tip speed ratio. In *Fundamental and advanced topics in wind power*. InTech.

Rezaei, V. (2015). Advanced control of wind turbines: Brief survey, categorization, and challenges. In *2015 American Control Conference (ACC)*, 3044–3051.

Rosyadi, M., Muyeen, S.M., Takahashi, R., and Tamura, J. (2012). Stabilization of fixed speed wind generator by using variable speed pm wind generator in multi-machine power system. In *2012 15th International Conference on Electrical Machines and Systems (ICEMS)*, 1–6.

Safari, B. (2011). Modeling wind speed and wind power distributions in rwanda. *Renewable and Sustainable Energy Reviews*, 15(2), 925–935.

Saravanakumar, R. and Jena, D. (2016). Nonlinear control of wind turbine with optimal power capture and load mitigation. *Energy Systems*, 7(3), 429–448.

Schlipf, D., Schlipf, D.J., and Kühn, M. (2013). Nonlinear model predictive control of wind turbines using lidar. *Wind energy*, 16(7), 1107–1129.

Simani, S. and Castaldi, P. (2018). Robust control examples applied to a wind turbine simulated model. *Applied Sciences*, 8(1), 29.

Singh, N., Pratap, B., and Swarup, A. (2018). Robust control design of variable speed wind turbine using quantitative feedback theory. *Proceedings of the Institution of Mechanical Engineers, Part A: Journal of Power and Energy*, 232(6), 691–705.

Song, D., Yang, J., Dong, M., and Joo, Y.H. (2017). Model predictive control with finite control set for variable-speed wind turbines. *Energy*, 126, 564 – 572.

Yang, Y. and Tan, S.C. (2019). Trends and development of sliding mode control applications for renewable energy systems. *Energies*, 12(15), 2861.